

Which Experiences Are Influential for Your Agent? Policy Iteration with Turn-over Dropout

Takuya Hiraoka^{1,2} Takashi Onishi^{1,2} Yoshimasa Tsuruoka^{2,3}

Abstract

In reinforcement learning (RL) with experience replay, experiences stored in a replay buffer influence the RL agent’s performance. Information about the influence is valuable for various purposes, including experience cleansing and analysis. One method for estimating the influence of individual experiences is agent comparison, but it is prohibitively expensive when there is a large number of experiences. In this paper, we present PI+ToD as a method for efficiently estimating the influence of experiences. PI+ToD is a policy iteration that efficiently estimates the influence of experiences by utilizing turn-over dropout. We demonstrate the efficiency of PI+ToD with experiments in MuJoCo environments.

1. Introduction

In reinforcement learning (RL) with experience replay (Lin, 1992), the performance of the RL agent is influenced by a replay buffer. Experience replay is a data-generating mechanism indispensable in modern off-policy RL methods (Mnih et al., 2015; Hessel et al., 2018; Haarnoja et al., 2018a; Kumar et al., 2020b). It uses a replay buffer to store past experiences for an RL agent. The buffer has a substantial effect on the performance (e.g. return) of RL agent components (e.g. the policy) (Fedus et al., 2020). Thus, estimating the influence of a buffer has been one of the RL community’s primary interests.

Previous studies have estimated the influence of the **buffer (or overall experience) properties** by comparing agents (upper part of Fig. 1). Buffer properties include the buffer size (Zhang & Sutton, 2017; Liu & Zou, 2018; Yarats et al., 2021), on-policyness (Fedus et al., 2020; Kumar et al., 2022; Di-Castro et al., 2021; Liu et al., 2021; Nikishin et al., 2022), non-stationarity (Igl et al., 2021; Di-Castro

¹NEC Corporation ²National Institute of Advanced Industrial Science and Technology ³The University of Tokyo. Correspondence to: Takuya Hiraoka <takuya-h1@nec.com>.

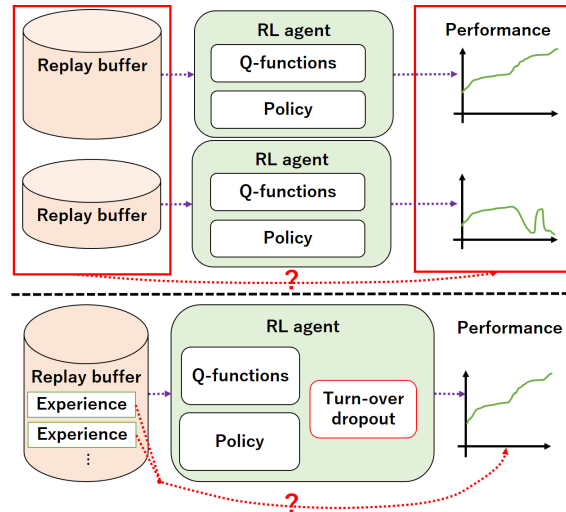


Figure 1: Comparison of our method, PI+ToD (lower part), with typical influence estimation methods for RL (upper part). The typical methods estimate the influence of a replay buffer property (e.g., buffer size) on the RL agent’s performance (e.g., return) via agent comparison. In contrast, our method estimates the influence of individual experiences stored in the buffer by using turn-over dropout (ToD) (Kobayashi et al., 2020).

et al., 2022), and optimality (Fu et al., 2020). These studies estimated the influence by comparing the performance of agents trained with different buffer properties.

The previous studies did not focus on the influence of **experiences stored in the buffer**, although such influence information is useful. Many of the aforementioned buffer properties (e.g. on-policyness and optimality) are shaped by the experiences stored in the buffer; thus, experiences should also affect performance. What if we could quantify the influence of the experiences? Such information could be used for many purposes, e.g. experience cleansing and analysis. **Experience cleansing:** We could improve the performance of an agent by removing negatively influential experiences from the buffer or save computational memory by removing non-influential experiences. **Experience analysis:** We could analyse individual experiences with respect to their influence, and thereby gain insights for ensuring the safety of the learned agent, for modifying the task

(e.g. reward structure) design, for improving agent components, etc.

Despite the usefulness of experience influence information, estimating it by agent comparison is impractical. We can estimate the influence by comparing agents, which are prepared (or retrained) for each possible experience deletion. However, the replay buffer (set of experiences) is often quite large (e.g. $10^3 - 10^6$ (Haarnoja et al., 2018b)), so, in such cases, using the agent comparison method is prohibitively costly. This motivates us to develop an efficient method for estimating the influence of experiences.

In this paper, we present PI+ToD, a policy iteration (PI) that efficiently estimates the influence of experiences (lower part of Fig. 1). PI is a class of RL methods including many promising RL methods (e.g. Fujimoto et al. (2018); Haarnoja et al. (2018a)). We augment PI with turn-over dropout (ToD) (Kobayashi et al., 2020) to efficiently estimate the influence of experiences, and refer to the augmented method as PI+ToD (Section 3). We evaluate the efficiency of PI+ToD instances in estimating the influence of experiences in MuJoCo environments (Todorov et al., 2012) (Section 4).

Although our primary contribution is **presenting an efficient influence estimation method**, we also make the following important contributions.

1. Demonstrating the usefulness of experience influences: Nikishin et al. (2022) insightfully noted that RL agents overfitting to old experiences tend to not work well. However, it is unclear when overfitting starts and how it progresses during learning. This information is important, especially for determining when to amend overfitting agents. We show that the progression of overfitting can be captured by tracking the influence of experiences during learning (see the paragraph “**Experience influence analysis**” in Section 4.1). This demonstrates the usefulness of experience influence information.

2. Providing a method to suppress performance degradation of PI+ToD: We provide an implementation-level method to alleviate the performance degradation that is potentially caused by the introduction of ToD into PI (Sections 3.2 and 4.2). Such a method is important for PI+ToD applications. If PI+ToD compromises performance (e.g., return) for the ability of efficient influence estimation, its practical application is restricted.

2. Preliminaries

In Section 3, we will describe our PI method for efficiently estimating experience influence. As preliminaries for this, we explain (i) PI (and RL problems to which PI is applied) in Section 2.1, and (ii) the problem of efficient experience influence estimation in Section 2.2.

2.1. Reinforcement Learning and Policy Iteration

Reinforcement learning (RL). RL addresses the problem of an agent learning to act in an environment. The environment provides the agent with a state s . The agent responds by selecting an action a , and then the environment provides a reward r and the next state s' . This interaction between the agent and environment continues until the state reaches termination. The agent aims to find a policy $\pi : \mathcal{S} \times \mathcal{A} \rightarrow \mathbb{R}_+$ maximizing cumulative rewards (return).

Policy iteration (PI). PI is a method for solving RL problems. In PI, the policy and Q-functions are updated by iteratively performing policy evaluation and improvement. Many instances of policy improvement and evaluation have been proposed (e.g. Fujimoto et al. (2018); Haarnoja et al. (2018a)). In this paper, as an example, we follow the ones for soft actor-critic (SAC) (Haarnoja et al., 2018b): In **policy evaluation** for SAC, the Q-functions $Q_{\phi_1}, Q_{\phi_2} : \mathcal{S} \times \mathcal{A} \rightarrow \mathbb{R}$, parameterised by $\phi_i \in \{1, 2\}$, are updated to minimize the soft Bellman residual:

$$\arg \min_{\phi_i} \mathbb{E}_{(s,a,r,s') \sim \mathcal{D}, a' \sim \pi_{\theta}(\cdot|s')} \left[\begin{aligned} & \left(r + \gamma \left(\min_{i \in \{1,2\}} Q_{\phi_i}(s', a') - \alpha \log \pi_{\theta}(a'|s') \right) \right. \\ & \left. - Q_{\phi_i}(s, a) \right)^2 \end{aligned} \right], \quad (1)$$

where \mathcal{D} is a replay buffer containing the collected experiences. Temperature α balances exploitation and exploration and affects the stochasticity of the policy. In **policy improvement** for SAC, policy π_{θ} , parameterised by θ , is updated to minimize the following objective:

$$\arg \min_{\theta} \mathbb{E}_{s \sim \mathcal{D}, a \sim \pi_{\theta}(\cdot|s)} [\alpha \log \pi_{\theta}(a|s) - Q_{\phi_i}(s, a)]. \quad (2)$$

2.2. Problem Description: Efficient Estimation of Influence of Experiences

Given the policy and Q-functions updated by PI, we aim to estimate the influence of individual experiences on performance. Formally, letting e_j be the j -th experience stored in \mathcal{D} , we evaluate the influence of e_j as

$$L \left(Q_{\phi_i, \mathcal{D} \setminus \{e_j\}}, Q_{\phi_i, \mathcal{D} \setminus \{e_j\}}, \pi_{\theta, \mathcal{D} \setminus \{e_j\}}, \mathcal{D}_{\text{test}} \right) - L \left(Q_{\phi_i, \mathcal{D}}, Q_{\phi_i, \mathcal{D}}, \pi_{\theta, \mathcal{D}}, \mathcal{D}_{\text{test}} \right), \quad (3)$$

where L is a metric for evaluating the performance of the Q-functions and policy on test dataset $\mathcal{D}_{\text{test}}$; $Q_{\phi_i, \mathcal{D}}$ and $\pi_{\theta, \mathcal{D}}$ are the Q-functions and policies for which the parameters are updated on the basis of all experiences stored in \mathcal{D} ; and $Q_{\phi_i, \mathcal{D} \setminus \{e_j\}}$ and $\pi_{\theta, \mathcal{D} \setminus \{e_j\}}$ are the ones for which the parameters are updated with \mathcal{D} other than e_j . The performance metric (i.e. L) can be defined in accordance with

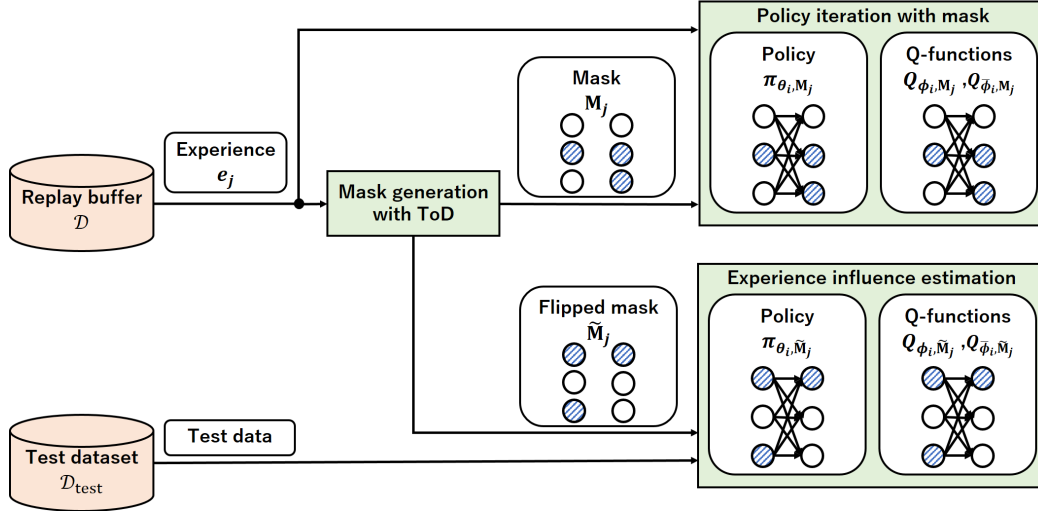


Figure 2: Concept of PI+ToD. Mask M_j and flipped mask \tilde{M}_j are generated using ToD for experience e_j . During policy iteration with e_j , M_j is applied to policy and Q-functions. M_j selects a unique subnetwork of the policy and Q-functions for e_j and limits e_j 's influence to within the subnetwork. For experience e_j influence estimation, \tilde{M}_j is applied to the functions. \tilde{M}_j selects a complement subnetwork, which is not influenced by e_j during PI.

one's own objective; we define it as **estimation bias** in our analyses in Section 4.1.

In practice, we need a method for efficiently estimating the influence of experiences (Eq. 3). We can estimate the influence by comparing agents that are prepared (or retrained) for each possible deletion of an experience. However, this requires training an agent by repeatedly executing PI (Eqs. 1 and 2) for each deletion case. This is computationally expensive and is infeasible for large \mathcal{D} . Therefore, we need a new method for efficiently estimating the influence of experiences without such agent comparison. We present such a method in the following section.

3. Proposed Method: Policy Iteration with Turn-over Dropout (PI+ToD)

In this section, we present **Policy Iteration with Turn-over Dropout (PI+ToD)** for efficiently estimating the influence of experiences. We first explain the concept of PI+ToD (Section 3.1) and then describe its practical implementation (Section 3.2).

3.1. Concept of PI+ToD

The concept of PI+ToD is shown in Fig. 2. PI+ToD generates a mask M_j and a flipped mask \tilde{M}_j for experience e_j (**Mask generation with ToD**). M_j is applied to the policy and Q-functions in PI with e_j (**Policy iteration with mask**). \tilde{M}_j is applied to the functions for estimating the influence of e_j (**Experience influence estimation**). The following paragraphs provide more details on these processes.

Mask generation with ToD. PI+ToD generates mask M_j

and flipped mask \tilde{M}_j for experience e_j using ToD. ToD is a variant of dropout (Srivastava et al., 2014) that generates mask M_j and flipped mask \tilde{M}_j . Similar to dropout, each element of M_j is randomly sampled from a Bernoulli distribution, and takes the value of $1/p$ or 0, with probabilities p and $1 - p$, respectively. However, unlike dropout, *the elements of M_j always take the same values when training with e_j* . This is achieved by specifying the random seed value uniquely assigned for the experience when generating a mask. We use j for the random seed value when generating M_j . Flipped mask \tilde{M}_j is the negation of M_j ; i.e. $\tilde{M}_j = 1 - M_j$. Mask M_j is used for PI, while the flipped mask \tilde{M}_j is used for influence estimation.

Policy iteration with mask. PI+ToD applies M_j to the policy and Q-functions in PI with e_j . It does this by using modified versions of policy evaluation (Eq. 1) and improvement (Eq. 2). The policy evaluation for PI+ToD is given by

$$\arg \min_{\phi_i} \mathbb{E}_{e_j = (s, a, r, s') \sim \mathcal{D}, a' \sim \pi_{\theta, \mathbf{M}_j}(\cdot | s')} \left[\begin{aligned} & \left(r + \gamma \left(\min_{i \in \{1, 2\}} Q_{\phi_i, \mathbf{M}_j}(s', a') - \alpha \log \pi_{\theta, \mathbf{M}_j}(a' | s') \right) \right. \\ & \left. - Q_{\phi_i, \mathbf{M}_j}(s, a) \right)^2 \end{aligned} \right]. \quad (4)$$

The policy improvement for PI+ToD is given by

$$\arg \min_{\theta} \mathbb{E}_{e_j = s \sim \mathcal{D}, a \sim \pi_{\theta, \mathbf{M}_j}(\cdot | s)} \left[\begin{aligned} & \alpha \log \pi_{\theta, \mathbf{M}_j}(a | s) - Q_{\phi_i, \mathbf{M}_j}(s, a) \end{aligned} \right]. \quad (5)$$

Here, Q_{ϕ_i, M_j} , $Q_{\bar{\phi}_i, M_j}$, and π_{θ_i, M_j} are the Q-functions, its target, and the policy, to which M_j is applied. In Eqs. 4 and 5, Q_{ϕ_i, M_j} and π_{θ_i, M_j} each use the same subnetworks selected by M_j when updated with e_j . As a result, only the subnetworks are updated and influenced by e_j . In other words, the complement subnetworks (the remaining networks) are not influenced by e_j . The complement subnetworks can be obtained by applying \tilde{M}_j to the policy and Q-functions. We utilize this property of the functions in experience influence estimation.

Experience influence estimation. PI+ToD estimates the influence of e_j by applying \tilde{M}_j to the policy and Q-functions. Specifically, it estimates the influence of e_j (Eq. 3) as

$$L\left(Q_{\bar{\phi}_i, \tilde{M}_j}, Q_{\phi_i, \tilde{M}_j}, \pi_{\theta_i, \tilde{M}_j}, \mathcal{D}_{\text{test}}\right) - L\left(Q_{\phi_i}, Q_{\bar{\phi}_i}, \pi_{\theta}, \mathcal{D}_{\text{test}}\right), \quad (6)$$

where the first term is the performance in the case of deletion of e_j , and the second term is the performance with all experiences; Q_{ϕ_i, \tilde{M}_j} and $\pi_{\theta_i, \tilde{M}_j}$ are the Q-functions and policy with \tilde{M}_j ; and Q_{ϕ_i} , $Q_{\bar{\phi}_i}$ and π_{θ} are the Q-functions and policy without masking.

This influence estimation method does not require preparing (or retraining) a policy and Q-functions for each case of experience deletion. This enables PI+ToD to efficiently estimate the influence of individual experiences. In Section 4.1, we evaluate the efficiency of PI+ToD in estimating experience influence.

3.2. Practical Implementation of PI+ToD

In the previous section, we described the concept of PI+ToD. In this section, we explain its practical implementation, i.e. (i) **instances of PI+ToD**, and (ii) our **implementation decisions**. These instances and decisions are used in our experiments (Section 4).

Instances of PI+ToD. In our experiments, we use SAC+ToD and its variants as PI+ToD instances. SAC+ToD uses SAC (Haarnoja et al., 2018a) for PI. The algorithm of SAC+ToD is presented in Algorithm 1. SAC+ToD differs from the original SAC in two primary ways: (i) it includes influence estimation based on Eq. 6 (lines 13–15), and (ii) the mask and flipped mask generated by ToD are applied to the policy and Q-functions. The mask is applied to the policy and Q-functions during policy evaluation (lines 6–8) and policy improvement (line 12). The flipped mask is applied to the policy and Q-functions during influence evaluation (line 15). Although we have explained SAC+ToD here, it is merely one PI+ToD instance. In Section 4, we evaluate other PI+ToD instances that use SAC variants.

Implementation decisions. We found that using ToD (i.e.

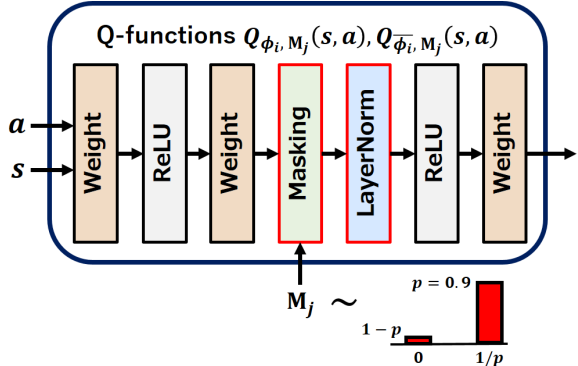


Figure 3: Implementation of Q-functions. Q-functions are implemented by modifying ones used in original SAC implementation (Haarnoja et al., 2018b). Modifications (highlighted in red) are adding a masking layer (Masking) and a layer normalization layer (LayerNorm). Masking layer masks input with M_j , elements of which are sampled from a Bernoulli distribution with probability $p = 0.9$. “Weight” is a weight layer, and “ReLU” is the activation layer of rectified linear units.

training with masks) degrades the performance of PI+ToD (Section 4.2). To alleviate this, we use (i) layer normalization and (ii) a high non-masking rate ($p = 0.9$), for both the policy and Q-functions. Our implementation of Q-functions is shown in Fig. 3¹.

Layer normalization: We apply layer normalization (Ba et al., 2016) following masking in accordance with the work of Hiraoka et al. (2022). This normalization contributes to suppressing performance degradation.

High non-masking rate: We found that (i) performance is greatly affected by the non-masking rate (i.e. p) and that (ii) using a sufficiently high rate ($p = 0.9$) suppresses the performance degradation.

These decisions to reduce the performance degradation of PI+ToD are important in practice. If PI+ToD requires a trade-off between performance and efficient influence estimation, its application would be limited. We will conduct experiments to validate the decisions in Section 4.2.

4. Experiments

We have described (i) PI+ToD as an efficient method for influence estimation (Section 3.1) and (ii) our implementation decisions (Section 3.2). In Section 4.1, we evaluate the efficiency of PI+ToD in estimating the influence of experiences on estimation bias. In Section 4.2, we evaluate the implementation decisions via an ablation study.

¹Our policy is also implemented by modifying the original one (Haarnoja et al., 2018b) in a similar manner

Algorithm 1 SAC+ToD (primary deviations from original SAC are highlighted in red)

- 1: Initialize policy parameters θ , Q-function parameters ϕ_1, ϕ_2 , and empty replay buffer \mathcal{D} .
 - 2: **repeat**
 - 3: Take action $a_t \sim \pi_\theta(\cdot|s_t)$; Observe reward r_t , next state s_{t+1} ; $\mathcal{D} \leftarrow \mathcal{D} \cup (s_t, a_t, r_t, s_{t+1})$.
 - 4: **for** G updates **do**
 - 5: Sample mini-batch $\mathcal{B} = \{e_j = (s, a, r, s')\}$ from \mathcal{D} , and **generate corresponding masks** $\{\mathbf{M}_j\}$.
 - 6: Compute target y :

$$y = r + \gamma \left(\min_{i=1,2} Q_{\bar{\phi}_i, \mathbf{M}_j}(s', a') - \alpha \log \pi_{\theta, \mathbf{M}_j}(a'|s') \right), \quad a' \sim \pi_{\theta, \mathbf{M}_j}(\cdot|s')$$
 - 7: **for** $i = 1, 2$ **do**
 - 8: Update ϕ_i with gradient descent using

$$\nabla_{\phi} \frac{1}{|\mathcal{B}|} \sum_{(s,a,r,s') \in \mathcal{B}} (Q_{\phi_i, \mathbf{M}_j}(s, a) - y)^2$$
 - 9: Update target networks with $\bar{\phi}_i \leftarrow \rho \bar{\phi}_i + (1 - \rho) \phi_i$.
 - 10: **end for**
 - 11: **end for**
 - 12: Update θ with gradient ascent using

$$\nabla_{\theta} \frac{1}{|\mathcal{B}|} \sum_{s \in \mathcal{B}} \left(\frac{1}{2} \sum_{i=1}^2 Q_{\phi_i, \mathbf{M}_j}(s, a) - \alpha \log \pi_{\theta, \mathbf{M}_j}(a|s) \right), \quad a \sim \pi_{\theta, \mathbf{M}_j}(\cdot|s)$$
 - 13: **Collect test dataset** $\mathcal{D}_{\text{test}}$
 - 14: **for** $e_j \in \mathcal{D}$ **do**
 - 15: **Generate corresponding flipped mask** $\tilde{\mathbf{M}}_j$ **and evaluate influence of** e_j **as**

$$L \left(Q_{\bar{\phi}_i, \tilde{\mathbf{M}}_j}, Q_{\phi_i, \tilde{\mathbf{M}}_j}, \pi_{\theta, \tilde{\mathbf{M}}_j}, \mathcal{D}_{\text{test}} \right) - L \left(Q_{\phi_i}, Q_{\phi_i}, \pi_{\theta}, \mathcal{D}_{\text{test}} \right)$$
 - 16: **end for**
-

4.1. Estimating Influence of Experience on Estimation Bias

We conduct an experiment to answer two questions: **Q1: How efficient is PI+ToD?** and **Q2: Can we obtain useful insights from experience influence information?** For this, we evaluate the efficiency of PI+ToD and analyse experiences influence, in four environments, on the task of “estimating the influence of experiences on estimation bias”, with three PI+ToD instances.

Environments. For evaluation, we use four MuJoCo (Todorov et al., 2012) environments: **Hopper**, **Walker2d**, **Ant**, and **Humanoid** (Brockman et al., 2016).

Task. We consider the task of estimating **the influence of experience** e_j **on estimation bias** defined as

$$\frac{\mathbb{E}_{(s,a,r,s') \sim \mathcal{D}_{\text{test}}} [Q_{\phi_i, \tilde{\mathbf{M}}_j}(s, a) - Q^\pi(s, a)]}{|\mathbb{E}_{(\bar{s}, \bar{a}) \sim \mathcal{D}_{\text{test}}} [Q^\pi(\bar{s}, \bar{a})]|} - \frac{\mathbb{E}_{(s,a,r,s') \sim \mathcal{D}_{\text{test}}} [Q_{\phi_i}(s, a) - Q^\pi(s, a)]}{|\mathbb{E}_{(\bar{s}, \bar{a}) \sim \mathcal{D}_{\text{test}}} [Q^\pi(\bar{s}, \bar{a})]|}, \quad (7)$$

where the first term represents an estimation bias in the case of e_j deletion, and the second term represents a vanilla es-

timization bias. Q^π represents the true Q-value under current policy π . Estimation bias has commonly been used to evaluate the performance of Q-functions (Hasselt et al., 2016; Fujimoto et al., 2018; Kumar et al., 2020a; Kuznetsov et al., 2020; Chen et al., 2021a). After every 1000 environment steps, we run test episodes and record the following information: (i) estimation bias (second term in Eq. 7), (ii) influence of experience on estimation bias (Eq. 7), and (iii) wallclock times required for experience influence estimation and for overall training. We also record (iv) a return as supplemental information.

PI+ToD instances. We evaluate experience influence estimation for three PI+ToD instances: **SAC+ToD**, **REDQ+ToD**, and **DroQ+ToD**. SAC+ToD is the method following Algorithm 1. REDQ+ToD is a method using REDQ (Chen et al., 2021a) for PI, and DroQ+ToD is a method using DroQ (Hiraoka et al., 2022) for PI. We use these instances to assess the difference in results induced by the difference in base PI methods.

Efficiency of PI+ToD instances (discussion for Q1). The times required for influence estimation (Fig. 4) show that all three PI+ToD instances efficiently estimate the influence of experiences. Fig. 4 shows that influence estimation

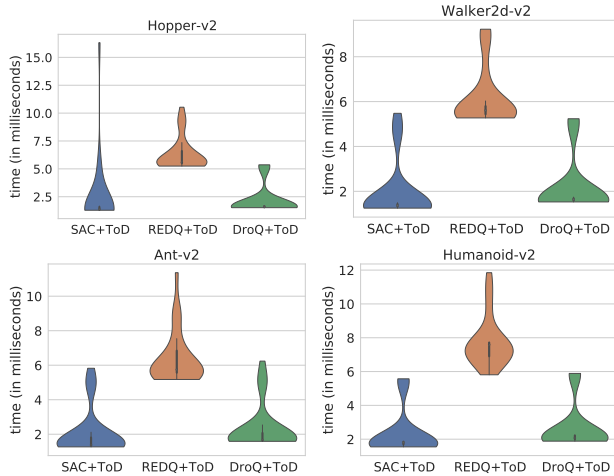


Figure 4: Distribution of time required for experience influence estimation, for the three PI+ToD instances, in four MuJoCo environments. The vertical axis represents time (in millisecond) required to estimate the influence of a single experience. The horizontal axis represents PI+ToD instances. These figures show that, on average, the influence estimation of an experience is computed within 10 ms.

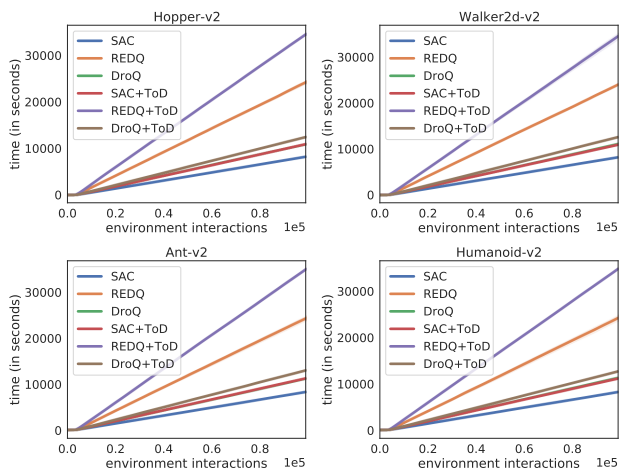


Figure 5: Training time of methods (baselines and PI+ToD instances). The vertical axis represents the total training time (in second). The horizontal axis represents number of environment steps (e.g. the number of executions of line 3 of Algorithm 1).

is performed within 10 ms per experience, on average, for all instances. This is much faster than the time required for an agent comparison method. A naive comparison method requires times similar to the ones shown in Fig. 5, per experience. For example, SAC requires about 8000 seconds to complete training corresponding to 10^5 environment steps in all environments.

Experience influence analysis (discussion for Q2). The estimation bias and the influence of experiences on it in Hu-

manoid are shown in Fig. 6. The figure indicates that *the instance that did not work well (i.e. SAC+ToD) is heavily influenced by old experiences*. Graphs for **Bias** and **Return** show that scores for SAC+ToD are worse than those for the other instances. Graphs for **Bias** show that the scores for the other instances converge toward near 0, whereas those for SAC+ToD do not. Furthermore, graphs for **Return** show that the scores for the other instances converge toward 3000 and 5000, whereas the scores for SAC+ToD converge toward approximately 500. Graphs for **Average experience influence on the bias** show that SAC+ToD is more heavily influenced by old experiences than the other instances. Here, experiences with scores (“average influence”) further away from zero have a heavier influence. SAC+ToD is heavily influenced by experience indexed to 0.0–0.4, while the other instances are heavily influenced by experiences indexed closer to 1.0. How does the influence of old experiences in SAC+ToD progress during training? The graph for **Experience influence in (SAC+ToD) seed 0** shows that (i) the influence of old experiences starts to increase at about 10^5 environment steps and that (ii) it becomes heavier as the number of steps increases. We also observe a similar tendency (“the instance that did not work well is heavily influenced by old experiences”) in Ant². The insight discussed in this paragraph suggests that SAC+ToD requires regularization to reduce its dependency on old experiences.

4.2. Ablation Study to Evaluate Implementation Decisions

In Section 3.2, we explained our implementation decisions for PI+ToD (i.e. using layer normalization and a high non-masking rate). In this section, we answer **Q3: Are our implementation decisions necessary?** For this, we conduct an ablation study for assessing their effectiveness.

We compare SAC, REDQ, DroQ, and their variants that use layer normalization and ToD with different unmasking rates. We denote the variants that use ToD with non-masking rate $p \in \{0.1, 0.3, 0.5, 0.7, 0.9\}$ alone, as SAC+ToD p , REDQ+ToD p , and DroQ+ToD p ³. We denote the variants that use both ToD and layer normalization as SAC+ToD p +LN, REDQ+ToD p +LN, and DroQ+ToD p +LN. We also denote variants that use layer normalization alone as SAC+LN and REDQ+LN⁴. We compare these methods, in four environments (Hopper, Walker, Ant, and Humanoid), in terms of return and esti-

²See results of SAC+ToD with seeds 0 and 2 in Figs. 11 and 15 in Appendix A

³DroQ uses layer normalization for Q-functions. Thus, for DroQ+ToD p , we do not apply layer normalization to the policy but do apply it to the Q-functions.

⁴We omit DroQ+LN because its performance is negligibly different from that of vanilla DroQ.

Which Experiences Are Influential for Your Agent

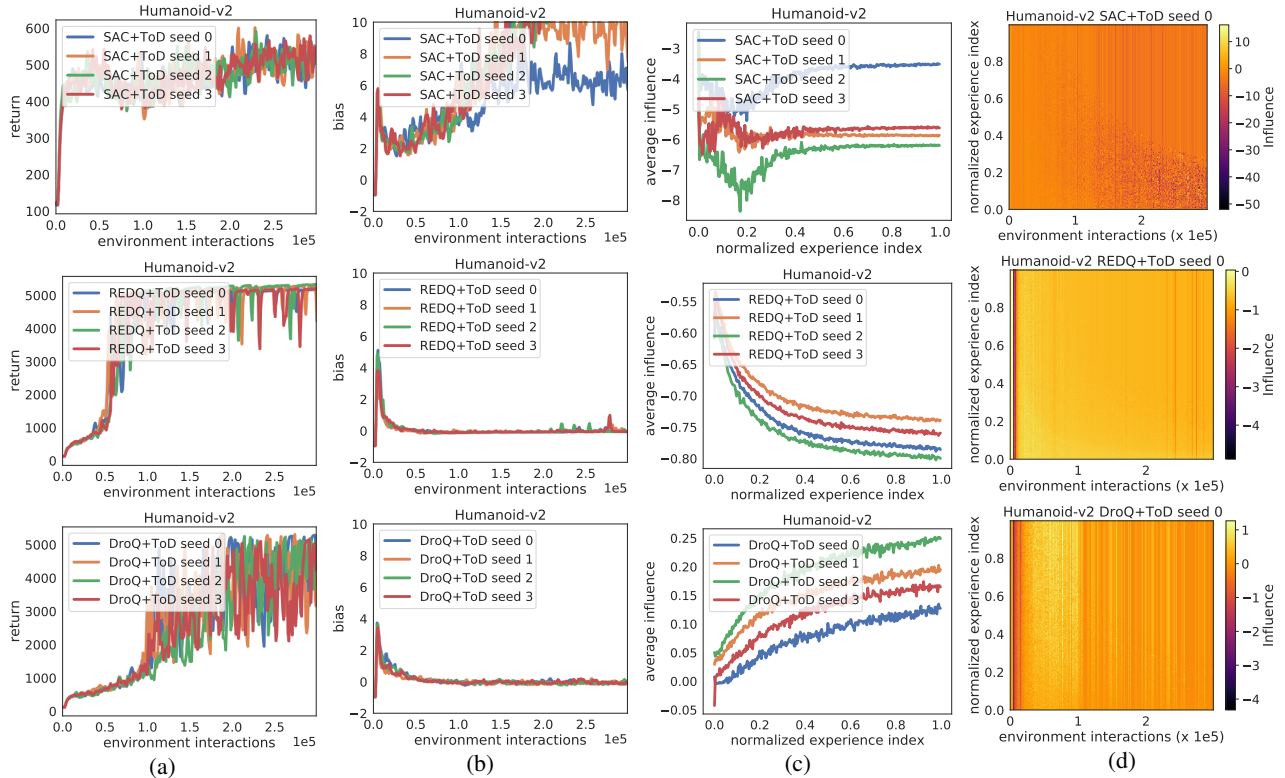


Figure 6: (a) **Return**, (b) **Bias**, (c) **Average influence on the bias**, and (d) **Experience influence in seed 0**, in Humanoid. **Return** and **Bias** show the progression of return and estimation bias in four trials with different random seeds. In these graphs, the vertical axis represents return and bias, respectively, and the horizontal axis represents the number of interactions with the environment. **Average influence on the bias** shows experience influence on estimation bias, averaged over environment interactions. The vertical axis represents the average experience influence, and the horizontal axis represents the normalized experience index ranging from 0.0 to 1.0. Here 0.0 represents the index for the oldest experience and 1.0 represents the index for the most recent experience. Finally, **Experience influence in seed 0** shows the progression of experience influence in trial with seed 0. These graphs indicate that *instance not working well (i.e. SAC+ToD)* is strongly influenced by old experiences. The results for all seeds and environments can be found in Appendix A.

mation bias.

Results (discussion for Q3). The results (Figs. 7 and 8) suggest that our implementation decisions suppress performance degradation. Regarding return (Fig. 7), using a high unmasking rate suppresses score degradation. For example, among REDQ+ToD0.1–0.9, REDQ+ToD0.9 achieves nearly the same score as REDQ, whereas the ones with smaller unmasking rates exhibit greater score degradation. Using layer normalization further suppresses score degradation. For example, REDQ+ToD0.9+LN achieves scores closer to REDQ’s score than REDQ+ToD0.9. Regarding estimation bias (Fig. 8), we can observe a similar trend.

5. Related Works

In this section, we review related studies and compare them with ours (Table 1).

Influence estimation in supervised learning (SL). Our

Table 1: Comparison between related studies and ours. We classify related studies into three categories (e.g. “Interpretable RL”) based on the basis of two criteria (e.g. “Applicable to RL?”)

	Applicable to RL?	Instance influence?
Influence estimation in SL	No	Yes
Agent comparison	Yes	No
Interpretable RL	Yes	No
Ours	Yes	Yes

study relates to previous studies for efficiently estimating the influence of training instances in the SL regime. In Section 3, we presented our method for efficiently estimating the influence of experiences (i.e. training instances). Methods that efficiently estimate the influence of training instances have been widely studied in the SL field. Most of them require supervised loss functions differentiable with respect to the parameters, for influence estimation (e.g. Koh & Liang (2017); Yeh et al. (2018); Hara et al. (2019);

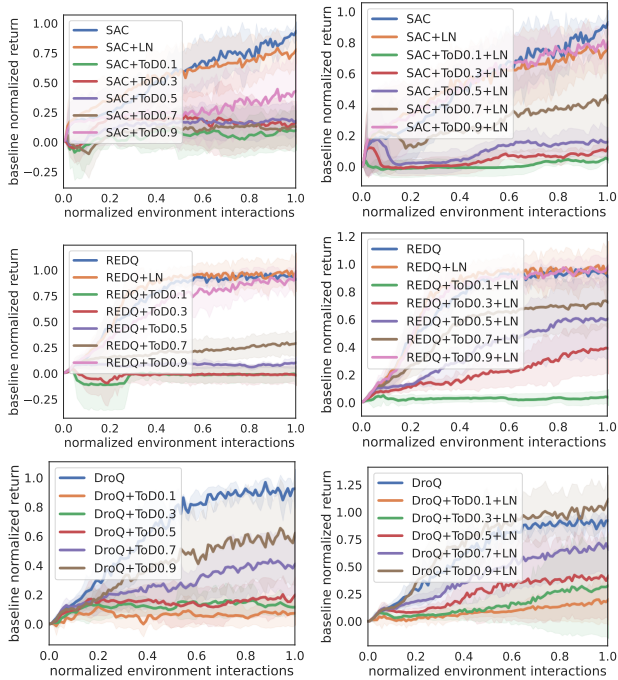


Figure 7: Summary of ablation study results (return). To summarize results over environments, we aggregate normalized scores of each method over environments. We normalize scores by dividing them by maximum score of corresponding baseline (SAC, REDQ, and DroQ). We then aggregate normalized scores by taking their average. The vertical axis represents average normalized score. The horizontal axis represents number of environment interactions normalized into $[0.0, 1.0]$. Here, 0.0 corresponds to zero environment interactions, and 1.0 corresponds to 1.25×10^5 interactions for Hopper and 3.0×10^5 interactions for the other environments. (Unnormalized scores for all environments are shown in Appendix B.1.)

Koh et al. (2019); Guo et al. (2020); Chen et al. (2021b); Schioppa et al. (2022)). These methods cannot be directly applied to our setting where such loss functions are unavailable. Unlike these methods, ToD (Kobayashi et al., 2020) estimates the influence without requiring a differentiable SL loss. Our work is based on ToD, but makes two non-trivial contributions: **Extending ToD to PI regime:** The original ToD is for the SL regime. To extend ToD to the PI regime, we modified it to apply masks to all parametric components appearing in PI (i.e. policy, target, and Q-functions) (Section 3.1). **Proposing a practical method:** We propose using a high non-masking rate and layer normalization to mitigate the performance degradation induced by ToD (Sections 3.2 and 4.2).

Agent comparison. Our study relates to previous studies that use agent comparison for estimating the influence of buffer properties (Zhang & Sutton, 2017; Liu & Zou, 2018; Yarats et al., 2021; Fedus et al., 2020; Kumar et al., 2022;

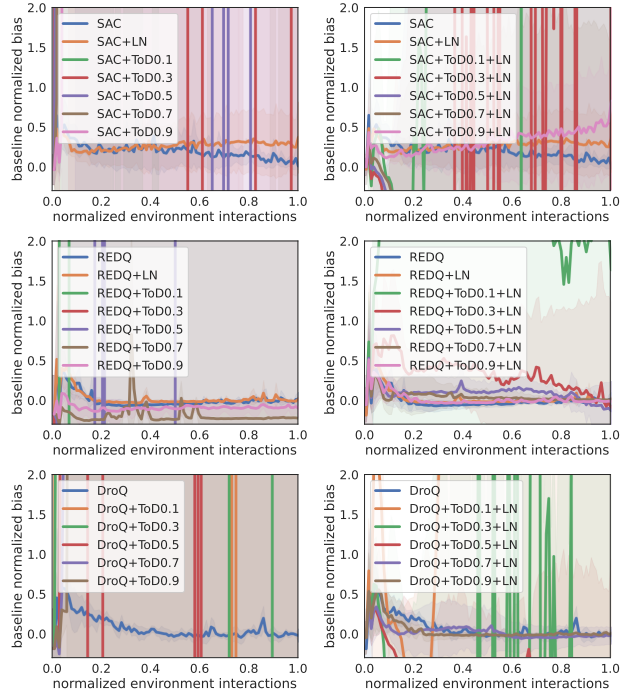


Figure 8: Summary of ablation study results (estimation bias). (Unnormalized scores are shown in Appendix B.2.)

Di-Castro et al., 2021; Liu et al., 2021; Nikishin et al., 2022; Igl et al., 2021; Di-Castro et al., 2022; Fu et al., 2020). In contrast to these studies, we use ToD for estimating the influence of the experiences stored in the buffer.

Interpretable RL. Our study relates to previous studies on interpretable (or explainable) RL methods. Our method (Section 3) estimates the influence of experiences, providing interpretability⁵. Previous studies in the RL community have proposed interpretable methods based on symbolic (or relational) representation (Džeroski et al., 2001; Yang et al., 2018; Lyu et al., 2019; Garnelo et al., 2016; Andersen & Konidaris, 2017; Konidaris et al., 2018), interpretable proxy models (e.g. decision trees) (Degris et al., 2006; Liu et al., 2019; Coppens et al., 2019), and saliency explanation (Zahavy et al., 2016; Greydanus et al., 2018; Mott et al., 2019; Wang et al., 2020; Anderson et al., 2020). These studies did not propose a method for estimating experience influence, whereas our study does.

6. Conclusion

We proposed PI+ToD, a PI method that uses ToD for efficiently estimating the influence of experiences (Section 3). We demonstrated that it efficiently estimates the influence of experiences in MuJoCo environments (Section 4).

⁵According to the taxonomy of Arrieta et al. (2020), our method can be classified as a post-hoc explainability method.

References

- Andersen, G. and Konidaris, G. Active exploration for learning symbolic representations. In *Proc. NeurIPS*, 2017.
- Anderson, A., Dodge, J., Sadarangani, A., Juozapaitis, Z., Newman, E., Irvine, J., Chattopadhyay, S., Olson, M., Fern, A., and Burnett, M. Mental models of mere mortals with explanations of reinforcement learning. *ACM Transactions on Interactive Intelligent Systems*, 10(2):1–37, 2020.
- Arrieta, A. B., Díaz-Rodríguez, N., Del Ser, J., Bennetot, A., Tabik, S., Barbado, A., García, S., Gil-López, S., Molina, D., Benjamins, R., et al. Explainable artificial intelligence (XAI): Concepts, taxonomies, opportunities and challenges toward responsible ai. *Information fusion*, 58:82–115, 2020.
- Ba, J. L., Kiros, J. R., and Hinton, G. E. Layer normalization. *arXiv preprint arXiv:1607.06450*, 2016.
- Brockman, G., Cheung, V., Pettersson, L., Schneider, J., Schulman, J., Tang, J., and Zaremba, W. OpenAI Gym. *arXiv preprint arXiv:1606.01540*, 2016.
- Chen, X., Wang, C., Zhou, Z., and Ross, K. W. Randomized ensembled double Q-learning: Learning fast without a model. In *Proc. ICLR*, 2021a.
- Chen, Y., Li, B., Yu, H., Wu, P., and Miao, C. Hydra: Hypergradient data relevance analysis for interpreting deep neural networks. In *Proc. AAAI*, 2021b.
- Coppens, Y., Efthymiadis, K., Lenaerts, T., and Nowe, A. Distilling deep reinforcement learning policies in soft decision trees. In *Proc. IJCAI Workshop on Explainable Artificial Intelligence*, 2019.
- Degrís, T., Sigaud, O., and Wuillemin, P.-H. Learning the structure of factored markov decision processes in reinforcement learning problems. In *Proc. ICML*, 2006.
- Di-Castro, S., Di Castro, D., and Mannor, S. Sim and Real: Better Together. In *Proc. NeurIPS*, 2021.
- Di-Castro, S., Mannor, S., and Castro, D. D. Analysis of stochastic processes through replay buffers. In *Proc. ICML*, 2022.
- Džeroski, S., De Raedt, L., and Driessens, K. Relational reinforcement learning. *Machine learning*, 43(1):7–52, 2001.
- Fedus, W., Ramachandran, P., Agarwal, R., Bengio, Y., Laroche, H., Rowland, M., and Dabney, W. Revisiting fundamentals of experience replay. In *Proc. ICML*, 2020.
- Fu, J., Kumar, A., Nachum, O., Tucker, G., and Levine, S. D4RL: datasets for deep data-driven reinforcement learning. *arXiv preprint arXiv:2004.07219*, 2020.
- Fujimoto, S., Hoof, H., and Meger, D. Addressing function approximation error in actor-critic methods. In *Proc. ICML*, 2018.
- Garnelo, M., Arulkumaran, K., and Shanahan, M. Towards deep symbolic reinforcement learning. *arXiv preprint arXiv:1609.05518*, 2016.
- Greydanus, S., Koul, A., Dodge, J., and Fern, A. Visualizing and understanding atari agents. In *Proc. ICML*, 2018.
- Guo, H., Rajani, N. F., Hase, P., Bansal, M., and Xiong, C. Fastif: Scalable influence functions for efficient model interpretation and debugging. *arXiv preprint arXiv:2012.15781*, 2020.
- Haarnoja, T., Zhou, A., Abbeel, P., and Levine, S. Soft actor-critic: Off-policy maximum entropy deep reinforcement learning with a stochastic actor. In *Proc. ICML*, 2018a.
- Haarnoja, T., Zhou, A., Hartikainen, K., Tucker, G., Ha, S., Tan, J., Kumar, V., Zhu, H., Gupta, A., and Abbeel, P. Soft actor-critic algorithms and applications. *arXiv preprint arXiv:1812.05905*, 2018b.
- Hara, S., Nitanda, A., and Maehara, T. Data cleansing for models trained with sgd. In *Proc. NeurIPS*, 2019.
- Hasselt, H. v., Guez, A., and Silver, D. Deep reinforcement learning with double Q-learning. In *Proc. AAAI*, 2016.
- Hessel, M., Modayil, J., van Hasselt, H., Schaul, T., Ostrovski, G., Dabney, W., Horgan, D., Piot, B., Azar, M. G., and Silver, D. Rainbow: Combining improvements in deep reinforcement learning. In *Proc. AAAI*, 2018.
- Hiraoka, T., Imagawa, T., Hashimoto, T., Onishi, T., and Tsuruoka, Y. Dropout Q-functions for doubly efficient reinforcement learning. In *Proc. ICLR*, 2022.
- Igl, M., Farquhar, G., Luketina, J., Boehmer, W., and Whiteson, S. Transient non-stationarity and generalisation in deep reinforcement learning. In *Proc. ICLR*, 2021.
- Kingma, D. P. and Ba, J. Adam: A method for stochastic optimization. 2015.
- Kobayashi, S., Yokoi, S., Suzuki, J., and Inui, K. Efficient estimation of influence of a training instance. *arXiv preprint arXiv:2012.04207*, 2020.

- Koh, P. W. and Liang, P. Understanding black-box predictions via influence functions. In *Proc. ICML*, 2017.
- Koh, P. W. W., Ang, K.-S., Teo, H., and Liang, P. S. On the accuracy of influence functions for measuring group effects. In *Proc. NeurIPS*, 2019.
- Konidaris, G., Kaelbling, L. P., and Lozano-Perez, T. From skills to symbols: Learning symbolic representations for abstract high-level planning. *Journal of Artificial Intelligence Research*, 61:215–289, 2018.
- Kumar, A., Gupta, A., and Levine, S. DisCor: Corrective feedback in reinforcement learning via distribution correction. In *Proc. NeurIPS*, 2020a.
- Kumar, A., Zhou, A., Tucker, G., and Levine, S. Conservative Q-learning for offline reinforcement learning. In *Proc. NeurIPS*, 2020b.
- Kumar, A., Agarwal, R., Ma, T., Courville, A., Tucker, G., and Levine, S. DR3: Value-based deep reinforcement learning requires explicit regularization. In *Proc. ICLR*, 2022.
- Kuznetsov, A., Shvechikov, P., Grishin, A., and Vetrov, D. Controlling overestimation bias with truncated mixture of continuous distributional quantile critics. In *Proc. ICML*, 2020.
- Lin, L.-J. Self-improving reactive agents based on reinforcement learning, planning and teaching. *Machine learning*, 8(3):293–321, 1992.
- Liu, G., Schulte, O., Zhu, W., and Li, Q. Toward interpretable deep reinforcement learning with linear model U-trees. In *Proc. ECML-PKDD*, 2019.
- Liu, R. and Zou, J. The effects of memory replay in reinforcement learning. In *Proc. Allerton*, 2018.
- Liu, X.-H., Xue, Z., Pang, J., Jiang, S., Xu, F., and Yu, Y. Regret minimization experience replay in off-policy reinforcement learning. In *Proc. NeurIPS*, 2021.
- Lyu, D., Yang, F., Liu, B., and Gustafson, S. SDRL: interpretable and data-efficient deep reinforcement learning leveraging symbolic planning. In *Proc. AAAI*, 2019.
- Mnih, V., Kavukcuoglu, K., Silver, D., Rusu, A. A., Veness, J., Bellemare, M. G., Graves, A., Riedmiller, M., Fidjeland, A. K., Ostrovski, G., et al. Human-level control through deep reinforcement learning. *nature*, 518(7540):529–533, 2015.
- Mott, A., Zoran, D., Chrzanowski, M., Wierstra, D., and Jimenez Rezende, D. Towards interpretable reinforcement learning using attention augmented agents. In *Proc. NeurIPS*, 2019.
- Nikishin, E., Schwarzer, M., D’Oro, P., Bacon, P.-L., and Courville, A. The primacy bias in deep reinforcement learning. In *Proc. ICML*, 2022.
- Schioppa, A., Zablotskaia, P., Vilar, D., and Sokolov, A. Scaling up influence functions. In *Proc. AAAI*, 2022.
- Srivastava, N., Hinton, G., Krizhevsky, A., Sutskever, I., and Salakhutdinov, R. Dropout: A simple way to prevent neural networks from overfitting. *Journal of Machine Learning Research*, 15(56):1929–1958, 2014.
- Todorov, E., Erez, T., and Tassa, Y. MuJoCo: A physics engine for model-based control. In *Proc. IROS*, pp. 5026–5033. IEEE, 2012.
- Wang, Y., Mase, M., and Egi, M. Attribution-based saliency method towards interpretable reinforcement learning. In *Proc. AAAI-MAKE*, 2020.
- Yang, F., Lyu, D., Liu, B., and Gustafson, S. PEORL: integrating symbolic planning and hierarchical reinforcement learning for robust decision-making. In *Proc. IJCAI*, 2018.
- Yarats, D., Fergus, R., Lazaric, A., and Pinto, L. Mastering visual continuous control: Improved data-augmented reinforcement learning. *arXiv preprint arXiv:2107.09645*, 2021.
- Yeh, C.-K., Kim, J., Yen, I. E.-H., and Ravikumar, P. K. Representer point selection for explaining deep neural networks. In *Proc. NeurIPS*, 2018.
- Zahavy, T., Ben-Zrihem, N., and Mannor, S. Graying the black box: Understanding DQNs. In *Proc. ICML*, 2016.
- Zhang, S. and Sutton, R. S. A deeper look at experience replay. *arXiv preprint arXiv:1712.01275*, 2017.

A. Estimating Influence of Experience on Estimation Bias

A.1. Return, Estimation Bias, and Average Influence on Bias

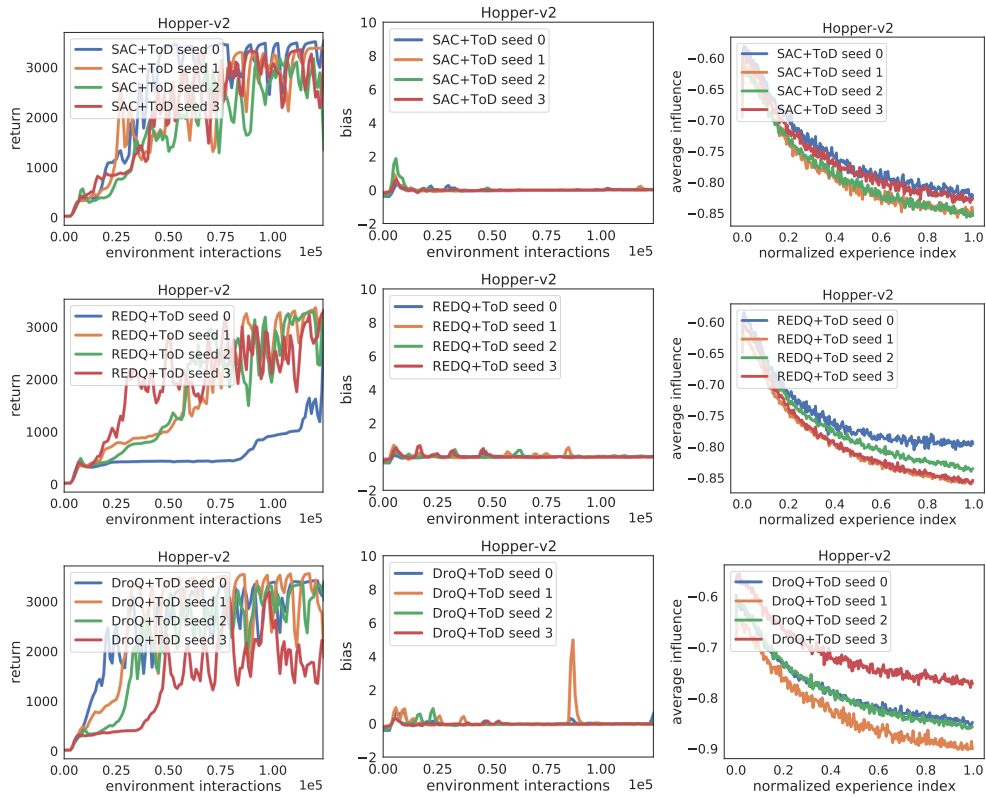


Figure 9: Return (first column from left), estimation bias (second from left), and average influence on bias (third from left), in Hopper.

Which Experiences Are Influential for Your Agent

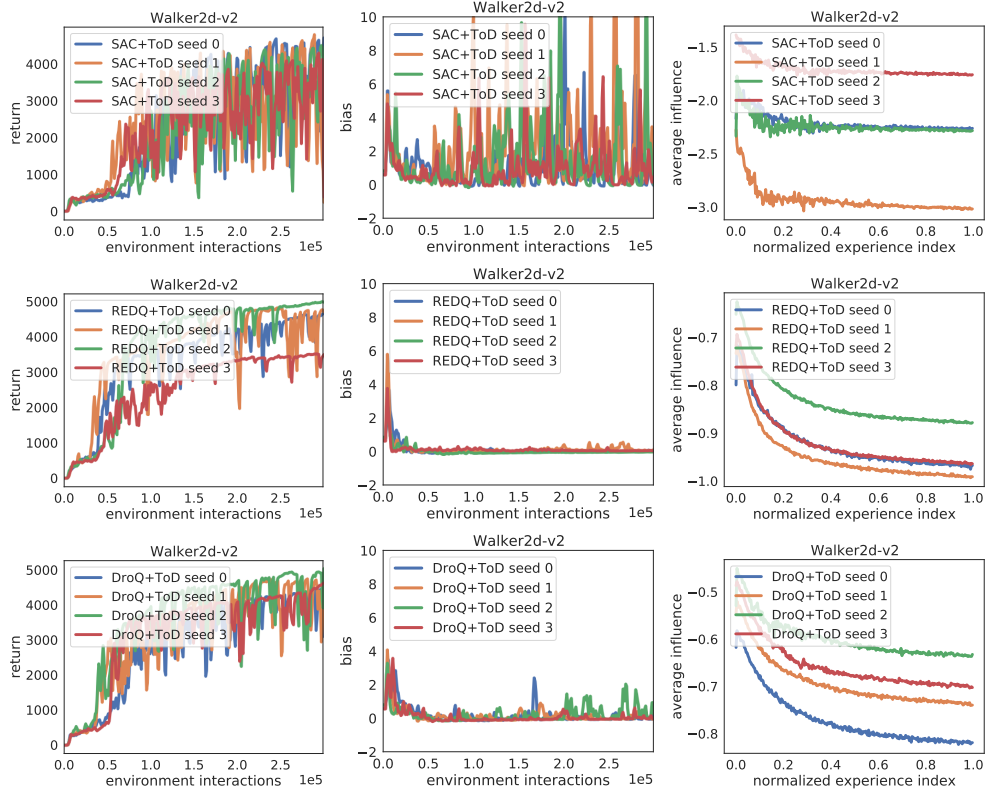


Figure 10: Return (first column from left), estimation bias (second from left), and average influence on bias (third from left), in Walker.

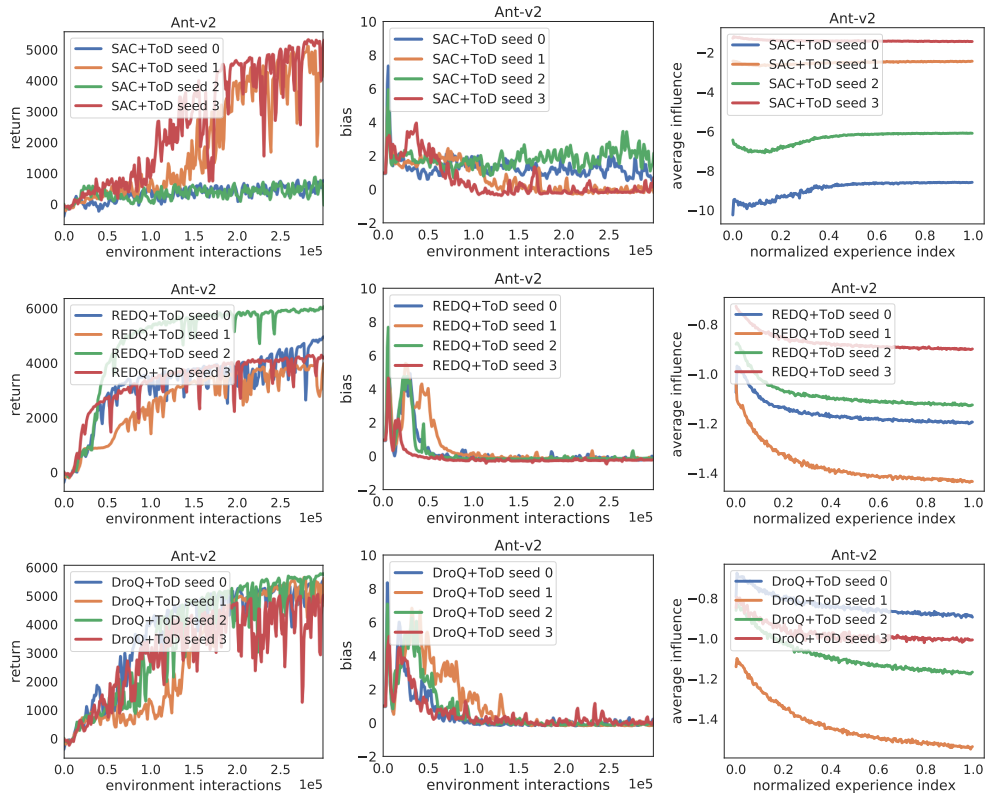


Figure 11: Return (first column from left), estimation bias (second from left), and average influence on bias (third from left), in Ant.

Which Experiences Are Influential for Your Agent

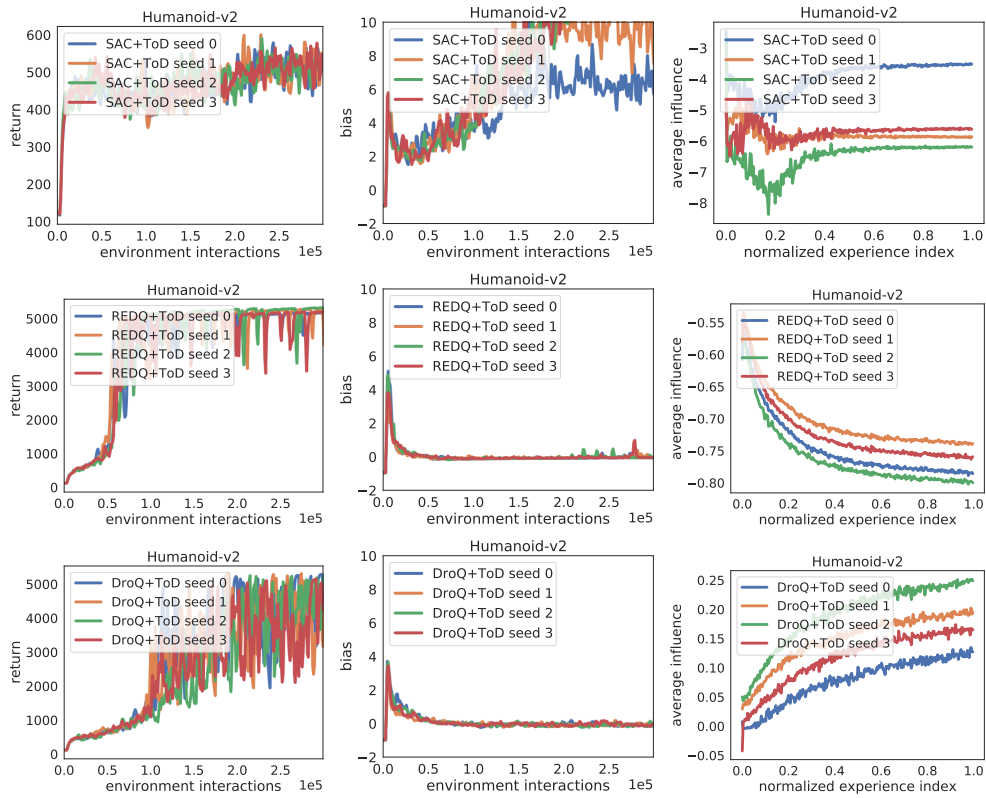


Figure 12: Return (first column from left), estimation bias (second from left), and average influence on bias (third from left), in Humanoid.

A.2. Influence of Experiences on Bias vs. Number of Environment Steps

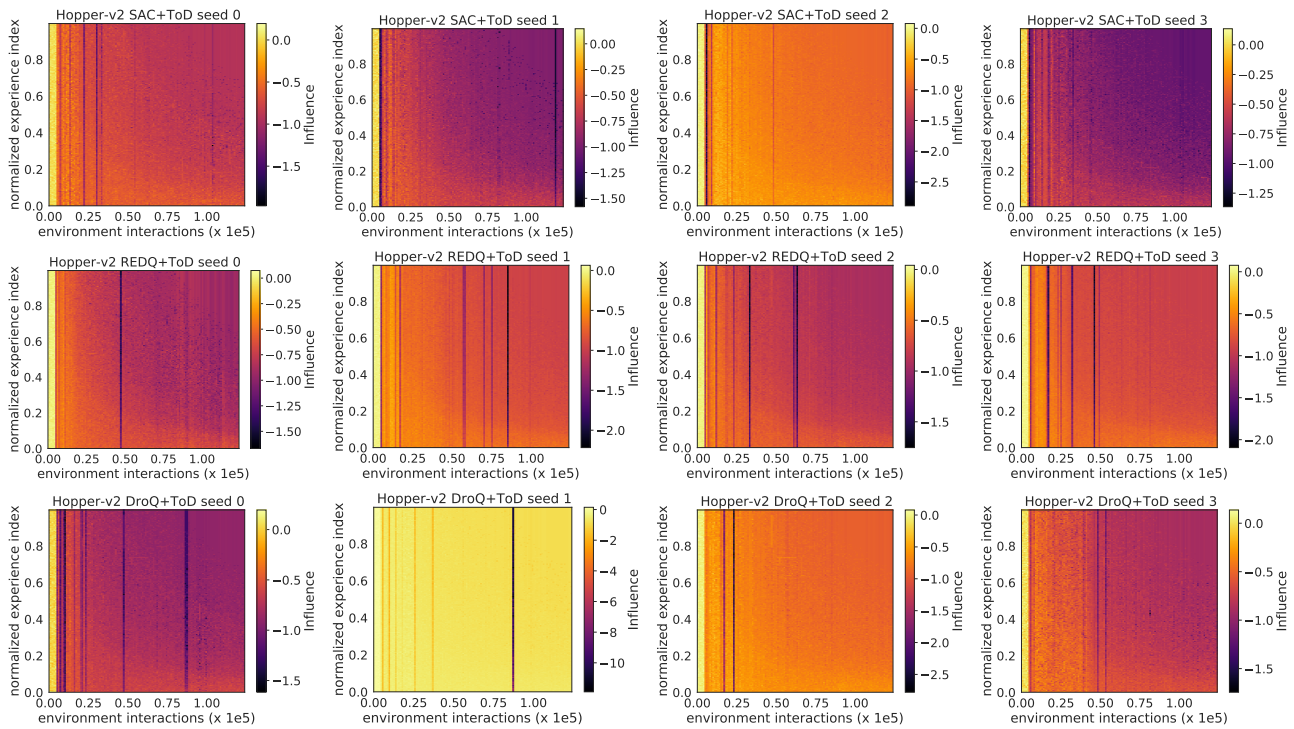


Figure 13: Influence of experiences for trials with random seeds 0, 1, 2, and 3, in Hopper.

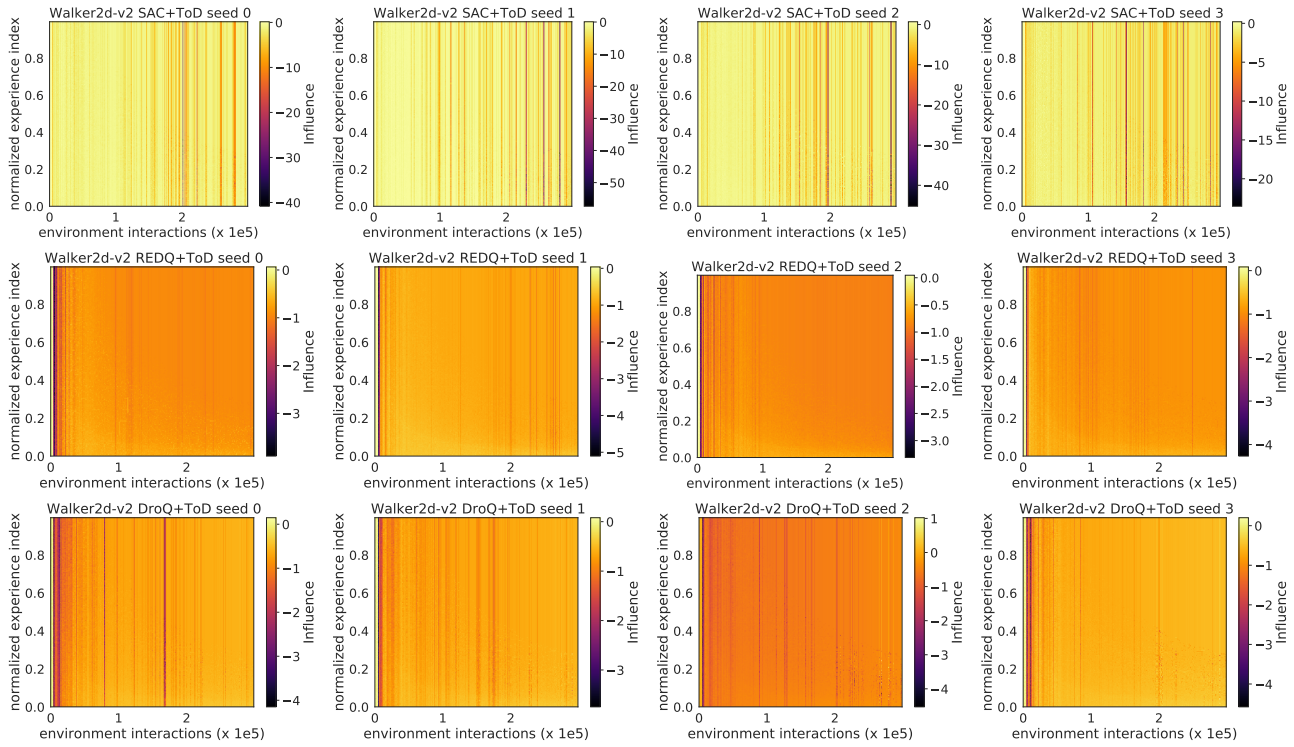


Figure 14: Influence of experiences for trials with random seeds 0, 1, 2, and 3, in Walker.

Which Experiences Are Influential for Your Agent

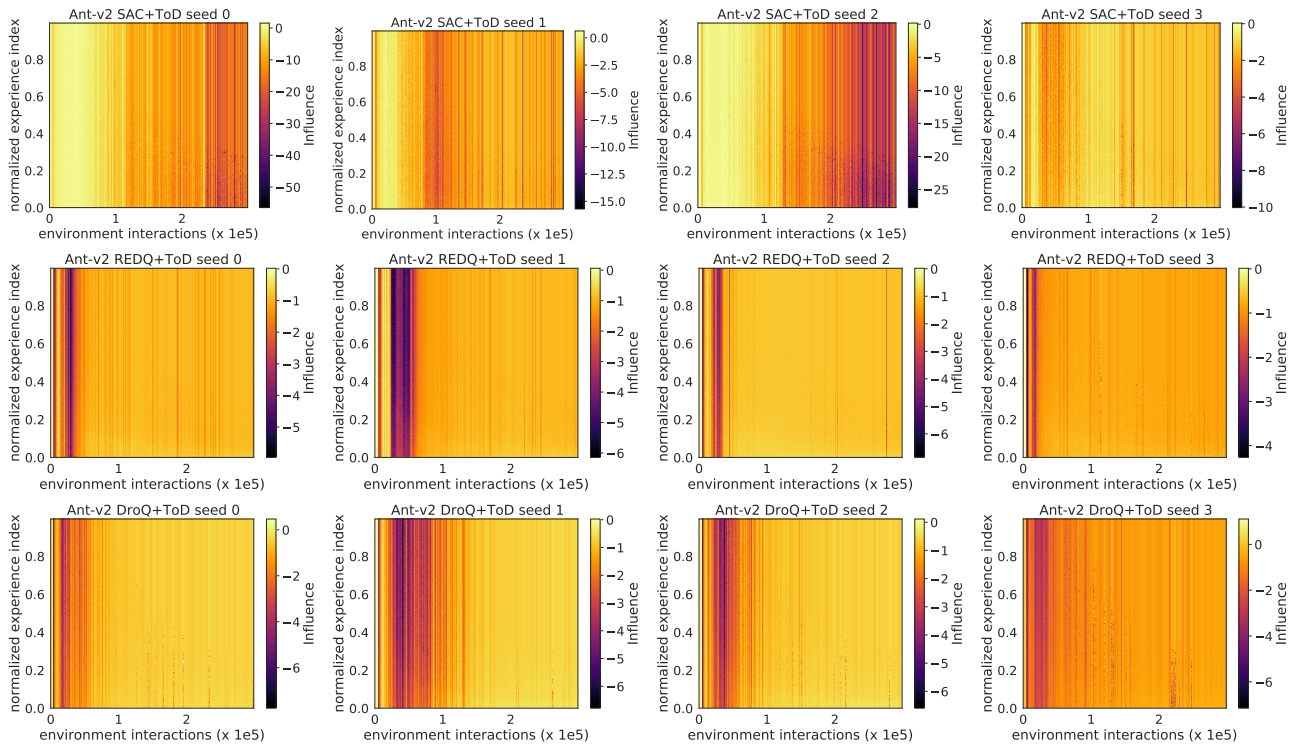


Figure 15: Influence of experiences for trials with random seeds 0, 1, 2, and 3, in Ant.

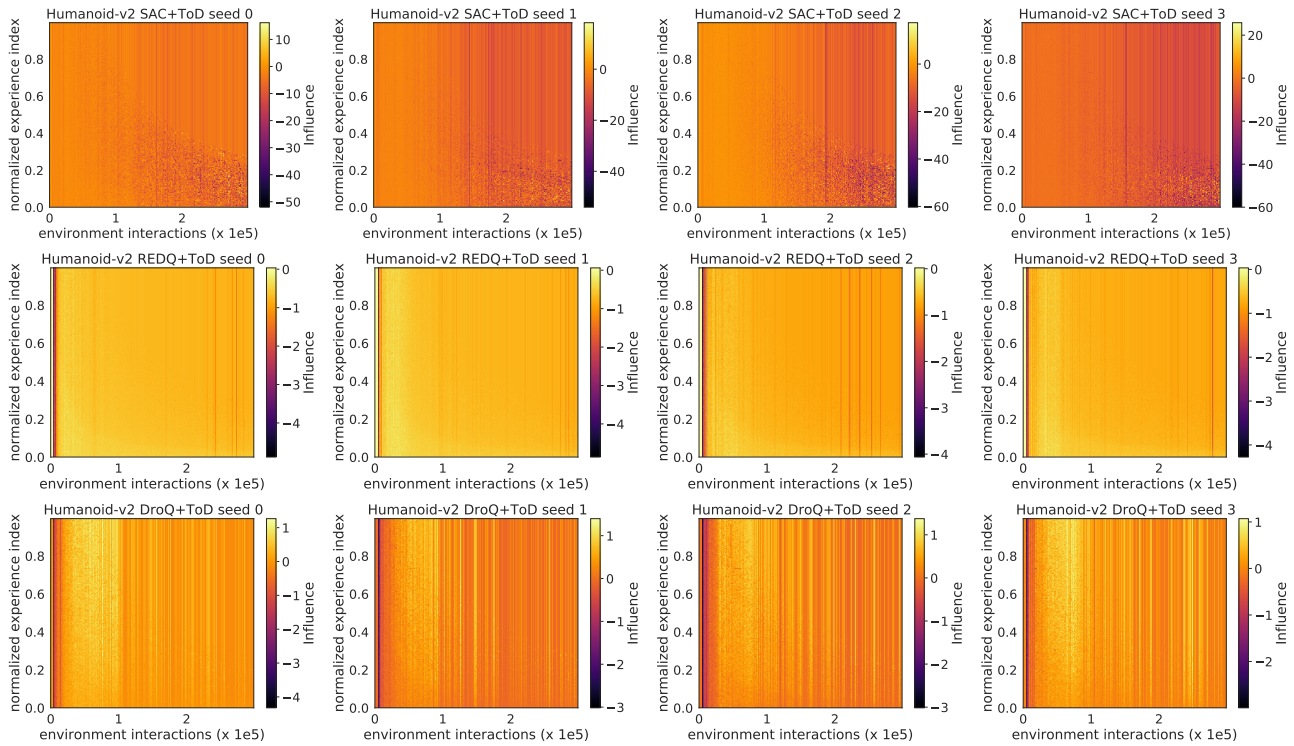


Figure 16: Influence of experiences for trials with random seeds 0, 1, 2, and 3, in Humanoid.

B. Ablation Studies for Our Implementation Decision

B.1. Average Return

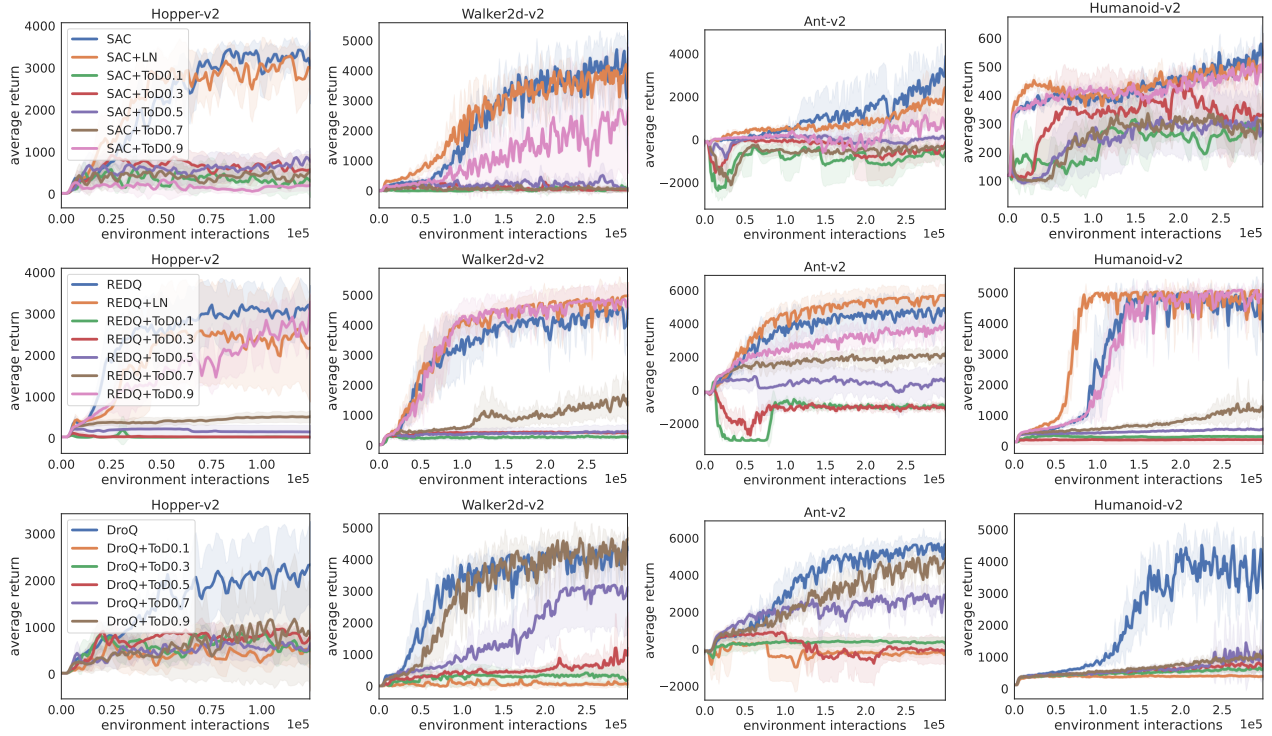


Figure 17: Ablation study result: effect of non-masking rate without layer normalization (average return). The horizontal axis represents the number of interactions with an environment. For each method, the average score for five independent trials is plotted as a solid line, and the standard deviation across trials is plotted as a transparent shaded region.

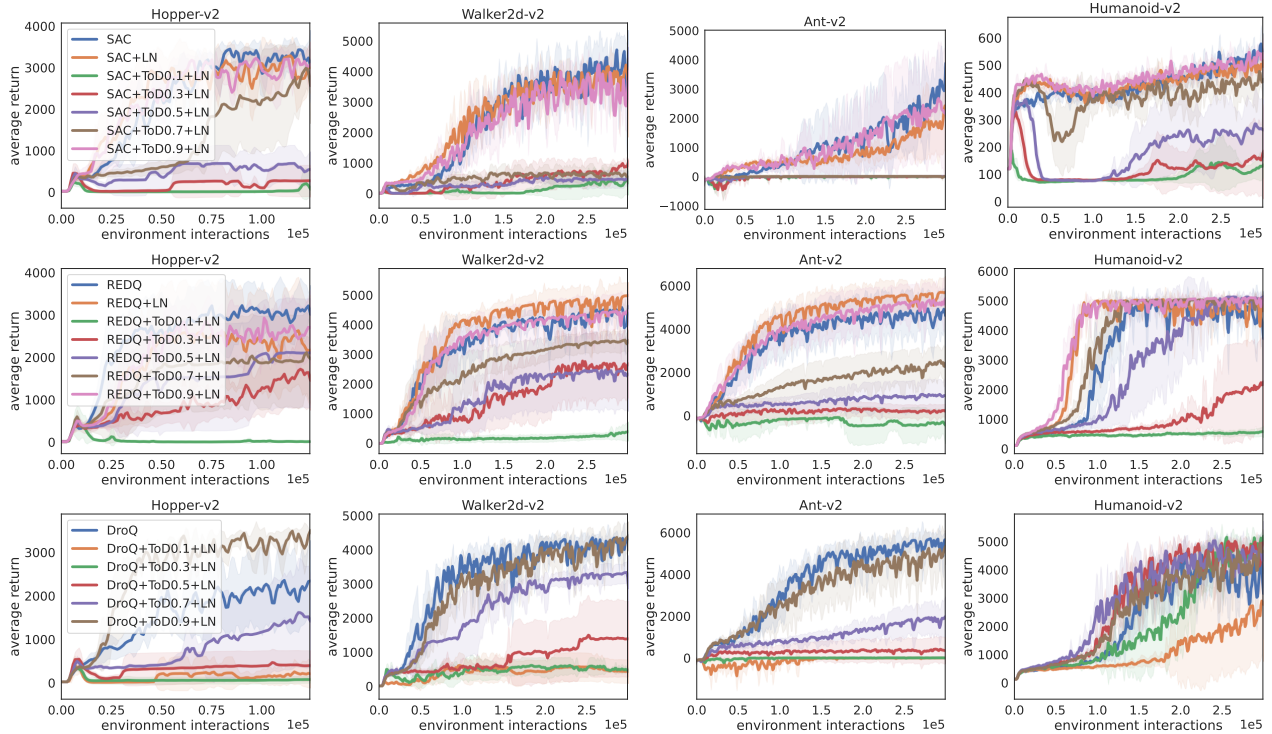


Figure 18: Ablation study result: effect of non-masking rate with layer normalization (average return).

B.2. Estimation Bias

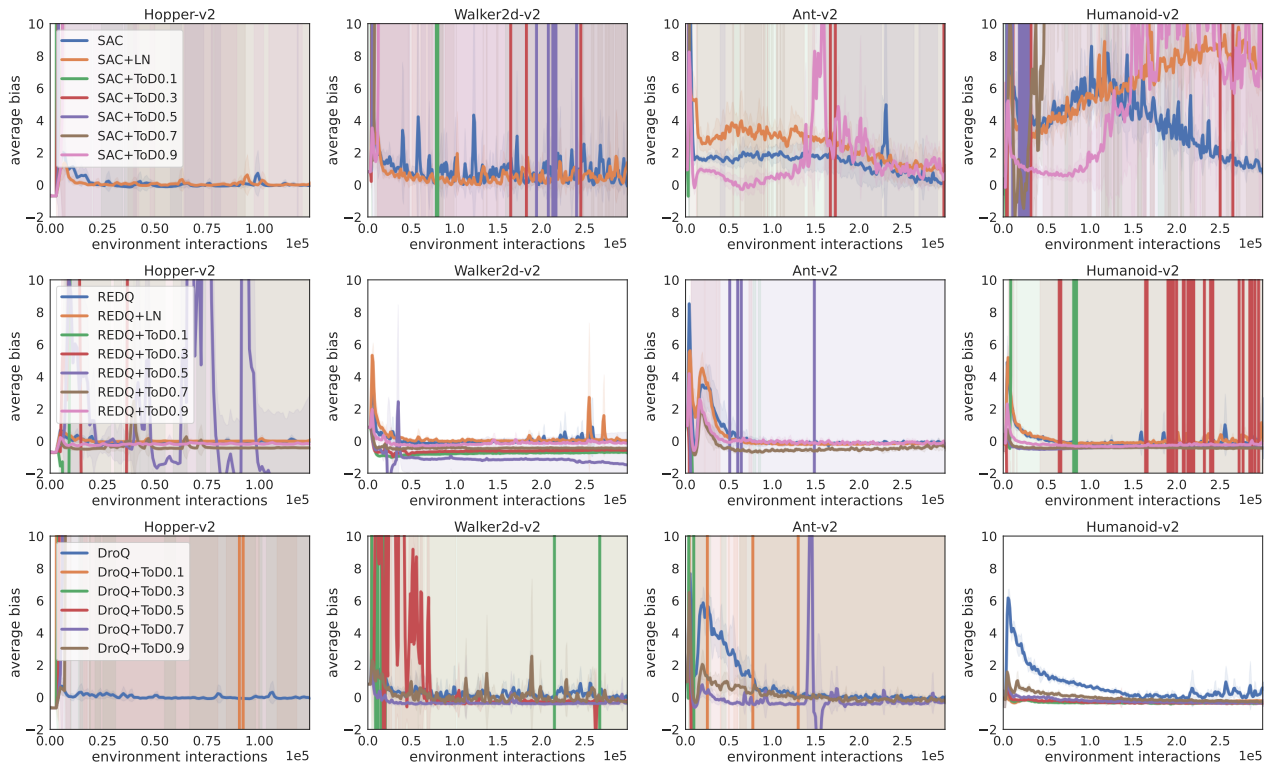


Figure 19: Ablation study result: effect of non-masking rate without layer normalization (estimation bias).

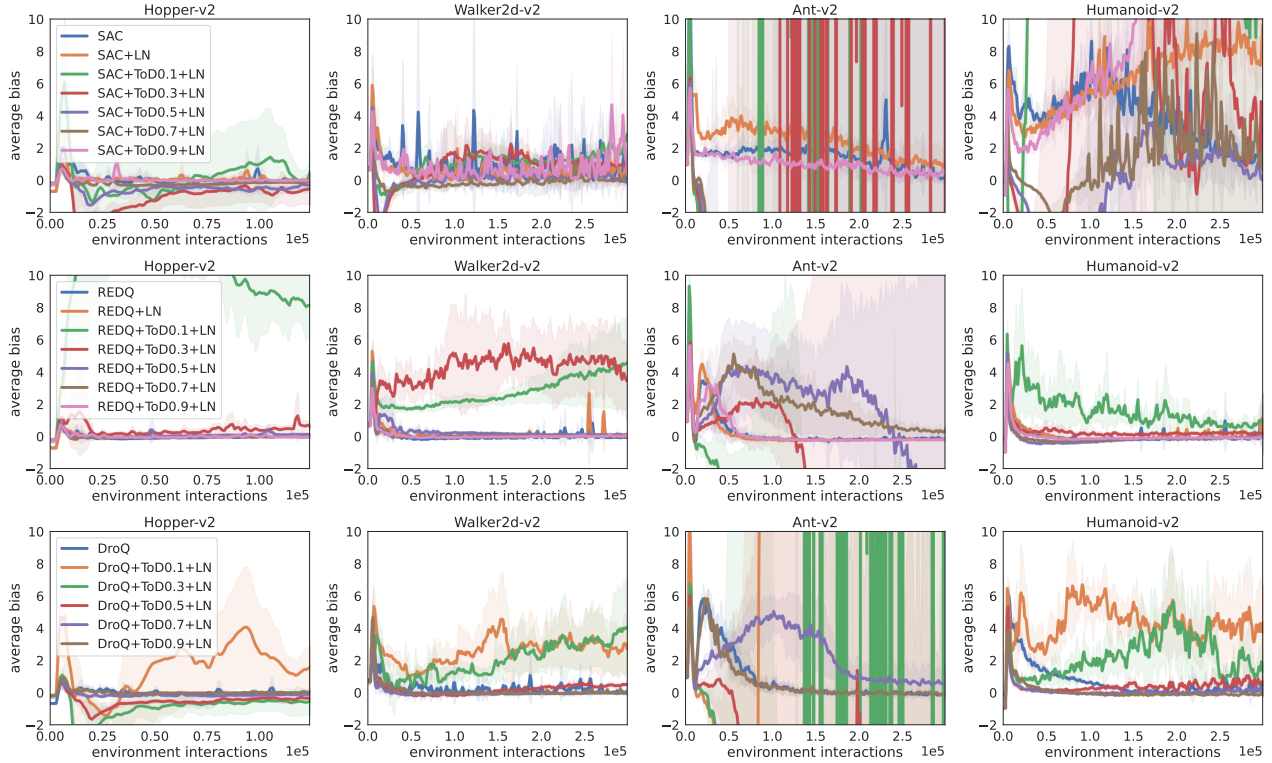


Figure 20: Ablation study result: effect of non-masking rate with layer normalization (estimation bias).

C. Computational Resources Used in Experiments

For our experiments described in Section 4.1, we used the ABCI compute node ⁶ equipped with two Intel Xeon Gold 6148 Processors 2.4 GHz (20 Cores) and four NVIDIA V100 GPUs. We ran four trials with different random seeds and assigned one GPU to each trial.

For our experiments in Section 4.2, we used a machine equipped with two Intel(R) Xeon(R) CPUs E5-2667 v4 and five NVIDIA Tesla K80. We ran five trials with different random seeds and assigned one GPU to each trial.

D. Hyperparameter Settings

The hyperparameter settings for each method, in the experiments discussed in Section 4, are listed in Table 2. Parameter values were set in accordance with Hiraoka et al. (2022).

Table 2: Hyperparameter settings

Method	Parameter	Value
SAC, REDQ, DroQ, SAC+ToD, REDQ+ToD, and DroQ+ToD	optimizer	Adam (Kingma & Ba, 2015)
	learning rate	$3 \cdot 10^{-4}$
	discount rate γ	0.99
	target-smoothing coefficient ρ	0.005
	replay buffer size	10^6
	number of hidden layers for all networks	2
	number of hidden units per layer	256
	mini-batch size	256
	random starting data	5000
	replay (update-to-data) ratio G	20
REDQ, DroQ, REDQ+ToD, and DroQ+ToD	in-target minimization parameter M	2
REDQ and REDQ+ToD	ensemble size N	10
DroQ and DroQ+ToD	dropout rate	0.0001 (Hopper)
		0.005 (Walker2d)
		0.01 (Ant)
		0.1 (Humanoid)
SAC+ToD, REDQ+ToD, and DroQ+ToD	non-masking rate p	0.9

E. Our Source Code

Our source code is available at <https://github.com/TakuyaHiraoka/Which-Experiences-Are-Influential-for-Your-Agent>

⁶<https://docs.abci.ai/en/job-execution/#compute-node-v>